A trip to the end of the universe and the twin "paradox"

Thomas Müller,[a] Andreas King, and Daria Adis
Institut für Astronomie und Astrophysik, Abteilung Theoretische Astrophysik, Auf der Morgenstelle 10, 72076 Tübingen, Germany

(Received 12 December 2006; accepted 8 December 2007)

Special relativity offers the possibility of going on a trip to the center of our galaxy or even to the end of our universe within a lifetime. On the basis of the well known twin paradox, we discuss uniformly accelerated motion and emphasize the local perspective of each twin concerning the interchange of light signals between both twins as well as their different views of the stellar sky. For this purpose we developed two Java applets that students can use to explore interactively and understand the topics presented here. © *2008 American Association of Physics Teachers.*
[DOI: 10.1119/1.2830528]

I. INTRODUCTION

The purpose of this article is to emphasize the local perspective of each twin in the well known twin paradox who can only do measurements with respect to his/her individual reference frame. This local perspective resembles Bondi's k-calculus[1] or the concept of radar time as discussed by Dolby and Gull,[2] where hypersurfaces of simultaneity are defined by local measurements of reflected light signals. The interesting information that both twins can interchange in our example are their individual proper times. They will not be able to determine the time dilation from this proper time because the information carrying the proper time of the other twin needs some time to travel the distance between them. This time interchange, as the motion itself, is not symmetric. Besides the time signals, both twins also receive light from distant stars or other astronomical sources. Depending on the relative velocity with respect to the light source, each twin will have a different view of the stellar sky because of aberration and the Doppler shift.

It is well known that acceleration is not crucial to explain the twin paradox.[3,4] (For a detailed discussion of the twin paradox we refer the reader to the standard literature.[5,6,8]) The crucial idea of the twin paradox is that there is an asymmetry between both twins. Only the difference in length of their paths makes the twins age at different rates. The traveling twin Tina leaves Earth with a rocket starting with zero velocity. Having reached her destination the twin might return to Earth. In order for the journey to be comfortable we consider a uniformly accelerated motion which is separated into four phases of equal duration. Even though acceleration is usually considered in conjunction with general relativity, it can also be treated within special relativity.[7–9]

We expect the reader to be familiar with basic calculations such as the Lorentz transformations and the description of acceleration within special relativity. In Sec. II we review the description of uniformly accelerated motion in special relativity. Following the example of Ruder[10] we present a special round trip consisting of four equal acceleration phases in Sec. III. From the local perspective taken in Sec. IV only time or light signals can be measured by each twin. As an example, we consider a flight to Vega and examine the time signal exchange in Sec. V. Because we stress the local perspective, we derive the frequency shift and aberration relations for the visualization of the stellar sky by means of a local reference frame (see Sec. VI). In Sec. VII we describe the visual effects due to aberration and the frequency shift. In the last section we show how far we can travel with the help of time dilation and length contraction.

In the appendix we give a short introduction to the Java applets: `TwinApplet` and `RelSkyApplet`.[11] The `TwinApplet` illustrates how far the traveling twin can go by means of relativistic time dilation and what time signals they can receive from each other. To use this applet we recommend reading Secs. II–V. The visualization of the stellar sky discussed in Sec. VII is realized in `RelSkyApplet`.

II. UNIFORM ACCELERATION

The earth twin Eric stays in the inertial reference frame S, while his traveling twin sister Tina leaves the Earth with constant acceleration α with respect to her own instantaneous system S'. All primed quantities refer to S', and unprimed quantities to S. From the Newtonian point of view, Tina will reach a velocity $v=\alpha\Delta t$ in the time Δt. She will then have covered a distance $\Delta x=\frac{1}{2}\alpha\Delta t^2$. Here, both twins will agree on time, velocity, and distance. In the theory of special relativity, both twins will still agree concerning time, velocity, and distance as long as Tina's velocity is much less than the speed of light, $v\ll c$. But in general, the earth twin Eric would measure an acceleration[5,8]

$$a=\alpha(1-\beta^2)^{3/2}=\frac{\alpha}{\gamma(\beta)^3}, \tag{1}$$

with $\beta=v/c$ and $\gamma=1/\sqrt{1-\beta^2}$, which is different to the Newtonian case. Given the initial velocity v_0, we obtain Tina's velocity v at time t by substituting $a=dv/dt$ in Eq. (1). The result is

$$v=\frac{\alpha t+c\zeta}{\sqrt{1+(\alpha t/c+\zeta)^2}}, \tag{2}$$

with $\zeta=\gamma(\beta_0)\beta_0$. The distance traveled $x=x(t)$ follows from Eq. (2) by another integration,

$$x=\frac{c^2}{\alpha}\left[\sqrt{1+\left(\frac{\alpha t}{c}+\zeta\right)^2}-\sqrt{1+\zeta^2}\right]+x_0, \tag{3}$$

where x_0 is the initial position at time $t=0$.

Time in both systems will go by at different rates depending on the relative velocity β,

$$dt'=\gamma(\beta)^{-1}dt. \tag{4}$$

Synchronizing at $t=t'=0$ gives

$$t' = \frac{c}{\alpha}\left[\operatorname{arcsinh}\left(\frac{\alpha t}{c} + \zeta\right) - \operatorname{arcsinh}\,\zeta\right], \tag{5}$$

or

$$t = \frac{c}{\alpha}\left[\sinh\left(\frac{\alpha t'}{c} + \operatorname{arcsinh}\,\zeta\right) - \zeta\right]. \tag{6}$$

For $\beta_0=0$ Eq. (6) simplifies to

$$t = \frac{c}{\alpha}\sinh\frac{\alpha t'}{c}. \tag{7}$$

If the traveling twin starts at $x_0=0$, her current position $x=x(t')$ is given by

$$x = \frac{c^2}{\alpha}\left(\cosh\frac{\alpha t'}{c} - 1\right). \tag{8}$$

Tina's velocity with respect to her proper time t' follows from Eqs. (7) and (2),

$$v = c\tanh\frac{\alpha t'}{c}. \tag{9}$$

Hence, because $|\tanh(x)| \leq 1$, the locally measured speed is always less than the speed of light in accordance with special relativity.

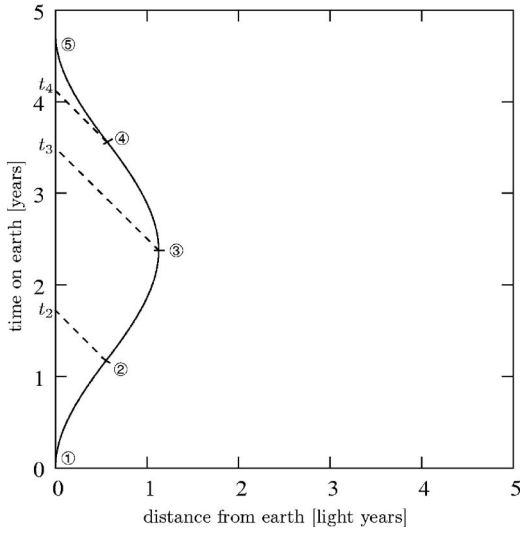

Fig. 1. Tina's journey is separated into four phases. She starts from point ①, accelerates up to maximum velocity at point ②, and slows down until she reaches the turning point ③. Then she accelerates in the opposite direction and slows down again until she comes home. Signals that were emitted by Tina in the accelerating phase i reach the Earth twin Eric in the interval $[t_i, t_{i+1}]$.

III. A SPECIFIC ROUND TRIP

The case we will investigate is discussed in several standard textbooks on special relativity, but not in as much detail.[1,5,10]

While Eric stays at home, Tina goes on a journey that is separated into four phases each of which last time T'. In the first phase she starts at space-time point ① and accelerates with α until she reaches the maximum velocity

$$v_{\max} = c\tanh\frac{\alpha T'}{c} \tag{10}$$

at point ②. Next, she decelerates with $-\alpha$ until she stops at her destination ③ where she has covered the distance

$$x_{\max} = 2\frac{c^2}{\alpha}\left(\cosh\frac{\alpha T'}{c} - 1\right). \tag{11}$$

The same procedure, but now in the opposite direction, brings Tina back home. Thus, the whole trip takes $4T'$ with respect to Tina's proper time, whereas Eric has to wait the time

$$4T = 4\frac{c}{\alpha}\sinh\frac{\alpha T'}{c} \tag{12}$$

for his sister's return. Hence, the bigger the acceleration and the longer the journey lasts, the bigger is the effect of time dilation and the different aging of both twins. Tina's worldline is shown in a spacetime diagram in Fig. 1, where Eric's proper time ct is plotted versus the distance x between Tina and Eric.

IV. OBSERVATION OF TIME SIGNALS

In contrast to usual discussions of special relativity concerning length contraction or time dilation with a group of synchronized observers, we concentrate on a local perspective. Hence, we can only use light signals exchanged by both twins to determine the proper time in each case. To do so the signals are coded with the proper emission time t_{emit} or t'_{emit} which will be received by the other twin at observation time t'_{obs} or t_{obs}. This measured time is not the actual time of the other twin. Because of the finite speed of light, the signals need some time to travel the distance between both twins.

Eric's perspective. Eric observes at his proper time t_{obs} a signal sent from Tina. Because of the finite speed of light, the signal must have been emitted at Earth time t_{emit},

$$t_{\text{obs}} = t_{\text{emit}} + \frac{x(t_{\text{emit}})}{c}. \tag{13}$$

The difference between t_{obs} and t_{emit} is the time needed for the signal to travel from Tina's current position $x_{\text{emit}}=x(t_{\text{emit}})$ to the Earth. To determine the position x_{emit} we have to find out the interval of acceleration when Tina has emitted the signal (compare Fig. 1).

The border points t_i, $(i=2,3,4)$, of the intervals follow from conditions such as $t_2=t_{②}+x_{②}/c$, whereas t_5 follows from Eq. (12). Thus, we have

$$t_1 = 0, \tag{14a}$$

$$t_2 = \frac{c}{\alpha}\left(\sinh\frac{\alpha T'}{c} + \cosh\frac{\alpha T'}{c} - 1\right), \tag{14b}$$

$$t_3 = \frac{c}{\alpha}\left(2\sinh\frac{\alpha T'}{c} + 2\cosh\frac{\alpha T'}{c} - 2\right), \tag{14c}$$

$$t_4 = \frac{c}{\alpha}\left(3\sinh\frac{\alpha T'}{c} + \cosh\frac{\alpha T'}{c} - 1\right), \tag{14d}$$

$$t_5 = 4\frac{c}{\alpha}\sinh\frac{\alpha T'}{c}. \tag{14e}$$

Depending on the interval $[t_i, t_{i+1}]$ Eric receives signals from the accelerating phase i, where Tina's current position was $x_{\text{emit}}=x(t_{\text{emit}})$. In the first time interval t_1-t_2 we get from Eq. (3) with $x_0=0$,

$$t_{\text{obs}} = t_{\text{emit}} + \frac{x_{①-②}(t_{\text{emit}})}{c} \tag{15a}$$

$$= t_{\text{emit}} + \frac{c}{\alpha}\left(\sqrt{1+\frac{\alpha^2 t_{\text{emit}}^2}{c^2}} - 1\right). \tag{15b}$$

We solve Eq. (15b) for t_{emit} and substitute it into Eq. (5) with $\beta_0=0$ and find the observed signal time t'_{emit},

$$t'_{\text{emit}} = \frac{c}{\alpha}\,\text{arcsinh}\,\frac{\alpha t_{\text{emit}}}{c} = \frac{c}{\alpha}\ln\left(1+\frac{\alpha t_{\text{obs}}}{c}\right). \tag{16}$$

In the accelerating time interval t_2-t_4, Eric's observation time t_{obs} is related to the emission time t_{emit} via

$$t_{\text{obs}} = T + \tilde{t}_{\text{emit}} + \frac{x_{②-④}(\tilde{t}_{\text{emit}})}{c}, \tag{17}$$

where $\tilde{t}_{\text{emit}}=t_{\text{emit}}-T$ measures time from point ②. Tina's current position $x_{②-④}(\tilde{t}_{\text{emit}})$ follows from Eq. (3),

$$x_{②-④}(\tilde{t}_{\text{emit}}) = -\frac{c^2}{\alpha}\left(\sqrt{1+\left(\frac{-\alpha\tilde{t}_{\text{emit}}}{c}+\zeta\right)^2} - \sqrt{1+\zeta^2}\right) + \frac{c^2}{\alpha}\left(\sqrt{1+\frac{\alpha^2T^2}{c^2}}-1\right), \tag{18}$$

where $\zeta=\beta_0\gamma(\beta_0)$, and the velocity β_0 is given by

$$\beta_0 = \frac{\alpha T/c}{\sqrt{1+\alpha^2T^2/c^2}}. \tag{19}$$

From Eq. (17) we can determine $\tilde{t}_{\text{emit}}$ to be

$$\tilde{t}_{\text{emit}} = \frac{1}{2}\frac{2\xi\sqrt{1+\zeta^2}-\xi^2\alpha/c}{\sqrt{1+\zeta^2}+\zeta-\xi\alpha/c}, \tag{20}$$

with

$$\xi = t_{\text{obs}} - T - \frac{c}{\alpha}\left(\sqrt{1+\frac{\alpha^2T^2}{c^2}}-1\right). \tag{21}$$

Equation (5) gives the corresponding time $\tilde{t}'_{\text{emit}}$. Hence, Eric receives at his observation time t_{obs} the emission time $t'_{\text{emit}}=\tilde{t}'_{\text{emit}}+T'$.

In the last time interval t_4-t_5 Eric's observation time t_{obs} follows from

$$t_{\text{obs}} = \bar{t}_{\text{emit}} + 3T + \frac{x_{④-⑤}(\bar{t}_{\text{emit}})}{c}, \tag{22}$$

where $x_{④-⑤}(\bar{t}_{\text{emit}})$ equals $x_{②-④}(\tilde{t}_{\text{emit}})$ with the substitutions $\alpha\mapsto-\alpha$, $\zeta\mapsto-\zeta$, $\tilde{t}_{\text{emit}}\mapsto\bar{t}_{\text{emit}}$, and $\bar{t}_{\text{emit}}=t_{\text{emit}}-3T$. To obtain the emission time t_{emit} from t_{obs} we follow the same procedure as in the previous accelerating time interval.

Tina's perspective. Now we consider the opposite situation where Eric sends his proper time t_{emit} to Tina. The arrival time t'_{obs} of the signal follows from the intersection of the future light cone of Eric at time t_{emit} with Tina's world line,

$$t_{\text{obs}} = t_{\text{emit}} + \frac{x_{\text{obs}}}{c}. \tag{23}$$

In contrast to Eric's perspective the calculations are a bit more straightforward because we determine t_{emit} from t'_{obs}. While Tina is in the first accelerating phase ①-② her proper time t'_{obs} transforms into t_{obs} via Eq. (7). Thus, her position is given by

$$x_{\text{obs}} = \frac{c^2}{\alpha}\left(\cosh\frac{\alpha t'_{\text{obs}}}{c}-1\right), \tag{24}$$

and the signal from Eric which arrives at time t'_{obs} has the time signature

$$t_{\text{emit}} = \frac{c}{\alpha}\left(\sinh\frac{\alpha t'_{\text{obs}}}{c} - \cosh\frac{\alpha t'_{\text{obs}}}{c} + 1\right). \tag{25}$$

In the accelerating phase ②-④ we obtain $\tilde{t}_{\text{obs}}=t_{\text{obs}}-T$ from Eq. (6) with $\zeta=\sinh(\alpha T'/c)$ for the observation time $\tilde{t}'_{\text{obs}}=t'_{\text{obs}}-T'$. Thus, we have

$$t_{\text{obs}} = T - \frac{c}{\alpha}\left(\sinh\frac{\alpha(-t'_{\text{obs}}+2T')}{c} - \sinh\frac{\alpha T'}{c}\right). \tag{26}$$

Tina's position x_{obs} when she receives the signal is given by Eq. (3) which simplifies to

$$x_{\text{obs}} = -\frac{c^2}{\alpha}\left(\cosh\frac{\alpha(-t'_{\text{obs}}+2T')}{c} - 2\cosh\frac{\alpha T'}{c} + 1\right). \tag{27}$$

The same procedure also applies to the last accelerating phase ④-⑤ for which we find

$$t_{\text{obs}} = 3T + \frac{c}{\alpha}\left[\sinh\frac{\alpha(t'_{\text{obs}}-4T')}{c} + \sinh\frac{\alpha T'}{c}\right] \tag{28}$$

for the observation time, and

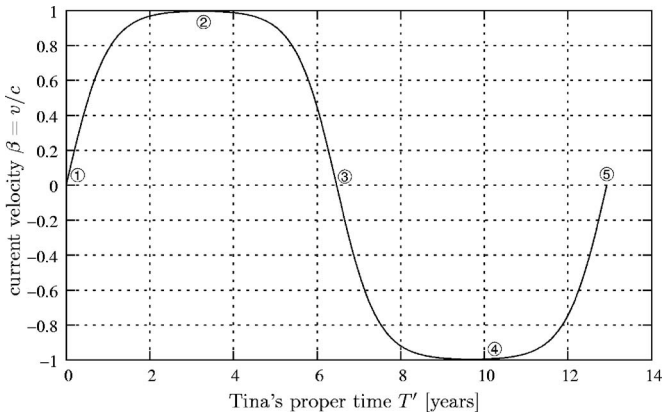

Fig. 2. Tina's current velocity for her flight to Vega and return to Earth with respect to her own proper time. The maximum speed $\beta\approx0.9975$ is reached at points ② and ④.

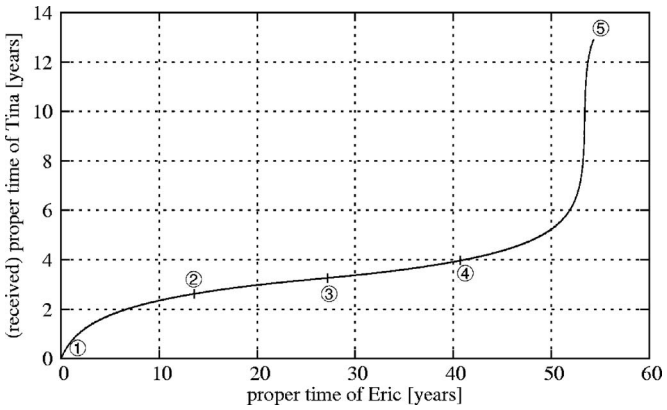

Fig. 3. The earth twin Eric sees/receives Tina's proper time t'_{emit} (ordinate) at his proper time t_{obs} (abscissa).

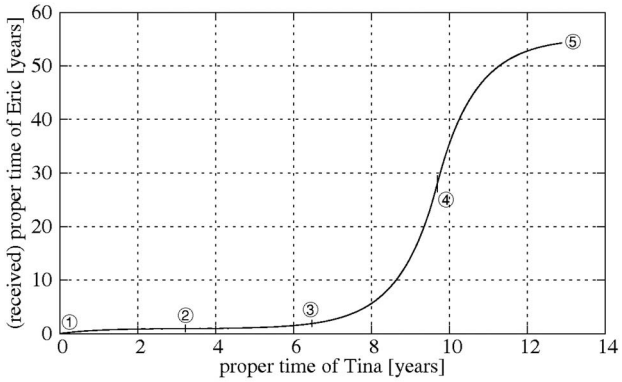

Fig. 5. The rocket twin Tina sees/receives Eric's proper time t_{emit} (ordinate) at her proper time t'_{obs} (abscissa).

$$x_{\text{obs}} = \frac{c^2}{\alpha}\left[\cosh\frac{\alpha(t'_{\text{obs}} - 4T')}{c} - 1\right] \tag{29}$$

for Tina's position. In both cases, the emission time t_{emit} follows from Eq. (23) with the corresponding time t_{obs} and position x_{obs}.

V. FLIGHT TO VEGA

As an example we consider a flight to our neighboring star Vega, which is roughly 25.3 ly away.[12] To be a most comfortable journey Tina accelerates with $\alpha = g \approx 9.81\ \text{m/s}^2$. While the journey takes $T'_{\text{total}} = 4T' \approx 12.93$ years with respect to her proper time, Eric has to wait $T_{\text{total}} \approx 54.48$ years for his sister to return. The worldline of Tina with respect to Eric's rest frame is shown in the spacetime diagrams, Figs. 4 and 6. Even though Tina follows an accelerated motion, her worldline is almost linear. Because of the moderate acceleration Tina's rocket needs roughly one year to reach 80% of the speed of light. At position $x_②$ she reaches maximum speed $\beta_{\max} \approx 0.9975$ (compare with Fig. 2).

Consider the exchange of time signals between both twins. The proper time sent by the one twin and received by the other is plotted in a time-time diagram (compare Figs. 3 and 5). The proper time of the twin who receives a signal is plotted on the abscissa and the proper time, which was sent by the other twin, is shown on the ordinate. The shapes of the curves are difficult to understand because two effects are mixed, time dilation and the nonlinear change of distance. To explain the differences between these curves, we also show the space-time diagram with Tina's worldline where the time signals are represented by straight lines with 45° slope (compare Figs. 4 and 6). Time intervals along Tina's worldline are not equally spaced because of her accelerated motion.

Eric's perspective (Figs. 3 and 4). While Eric stays at home, Tina leaves Earth with proper acceleration α. Because the distance between both twins grows, it is obvious that the signals emitted by Tina need more and more time to reach Eric. Also, because of time dilation, Tina seems to wait a longer time than expected before emitting the next signal. Even though Tina is already on the way back to home when

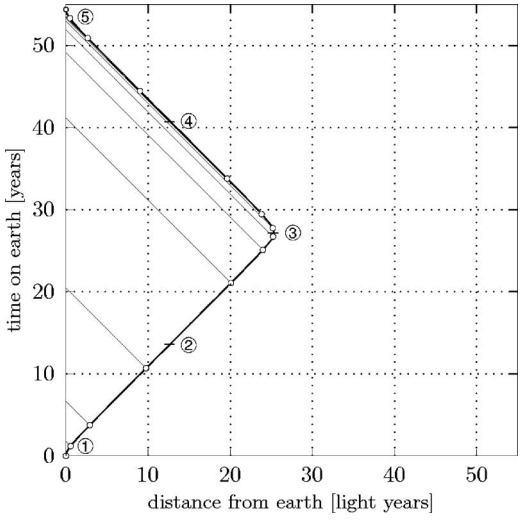

Fig. 4. Spacetime diagram for Tina's flight to Vega and return to Earth with respect to Eric's frame. At point ③ Tina reaches Vega and immediately returns. At ② and ④ she changes her acceleration direction. The small circles represent the events when Tina sends a time signal to Eric. They are separated by a single year with respect to her proper time t'. Note that the time units are not equally spaced on Tina's worldline.

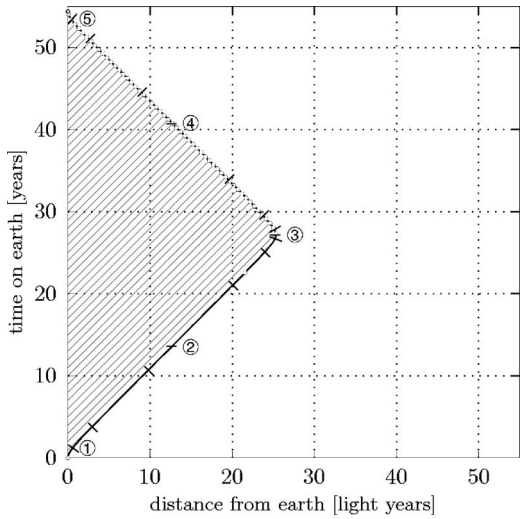

Fig. 6. The earth twin Eric sends a time signal every year with respect to his proper time t. The dashes on Tina's worldline mark the years of her proper time. Eric's first signal does not reach Tina until she already decelerates to her destination ③.

she has left her destination ③, Eric will collect most of her time signals only during the very end of her journey.

Eric observes at his proper time $t_{obs} \approx 20$ years a time signal which was sent by Tina at her proper time $t'_{emit} = 3$ y when she was 10 ly away from home. But her current position at Eric's observation time is $x \approx 19$ ly and her watch shows roughly 4 y.

Tina's perspective (Fig. 5 and 6). It might be obvious that Tina's perspective is different. Eric's "first year" signal reaches Tina only when she already decelerates to her destination ③. On her way home, Tina seems to receive the signals regularly, but because of time dilation she collects most of the signals around point ④ when she has maximum speed and the time dilation effect is strongest.

To investigate this situation for different proper accelerations α and different durations T', we have written the interactive Java applet `TwinApplet`.[11] A short description of the applet is given in Appendix A; a more detailed discussion as well as two examples can be found in the help menu of the applet.

VI. THE ACCELERATED REFERENCE FRAME

A. Aberration, Doppler shift and length contraction

In four-dimensional spacetime all observers have their own local reference system which is given by four base vectors. Each measurement is taken with respect to this local tetrad.

Consider the flat Minkowski spacetime which is represented by the metric

$$ds^2 = -c^2dt^2 + dx^2 + dy^2 + dz^2. \tag{30}$$

The local tetrad $\{\mathbf{e}_i\}_{(i=0,\ldots,3)}$ of an observer moving with velocity $\beta = v/c$ in the direction of the x axis reads

$$\mathbf{e}_0 = \gamma(\mathbf{e}_t + \beta\mathbf{e}_x), \quad \mathbf{e}_2 = \mathbf{e}_y, \tag{31a}$$

$$\mathbf{e}_1 = \gamma(\beta\mathbf{e}_t + \mathbf{e}_x), \quad \mathbf{e}_3 = \mathbf{e}_z, \tag{31b}$$

where $(\mathbf{e}_t, \mathbf{e}_x, \mathbf{e}_y, \mathbf{e}_z)$ are the four base vectors of an observer at rest with respect to the Minkowski coordinate system (30). Each base vector points in its positive coordinate direction, where $\mathbf{e}_0$ is adapted to the four-velocity $\mathbf{u}$ of the moving observer,

$$\mathbf{e}_0 = \frac{1}{c}\mathbf{u}. \tag{32}$$

The current four-velocity of the accelerated twin Tina at time t' is given by $\mathbf{u} = u^j\mathbf{e}_j, (j = t, x, y, z)$ with

$$u^t = c\frac{dt}{dt'} = c\gamma(\beta), \quad u^x = \frac{dx}{dt'} = \beta\gamma(\beta), \tag{33}$$

and $u^y = u^z = 0$. Her four-acceleration a^μ is

$$a^t = \frac{d^2t}{dt'^2} = \frac{\alpha}{c}\beta\gamma(\beta), \quad a^x = \frac{d^2x}{dt'^2} = \alpha\gamma(\beta), \tag{34}$$

and $a^y = a^z = 0$, where $\beta = \beta(t')$ is the relative velocity at Tina's proper time t'. Thus, her local tetrad at time t' is given by

$$\mathbf{e}_0^{S'}(t') = \cosh\frac{\alpha t'}{c}\mathbf{e}_t + \sinh\frac{\alpha t'}{c}\mathbf{e}_x, \quad \mathbf{e}_2^{S'}(t') = \mathbf{e}_y, \tag{35a}$$

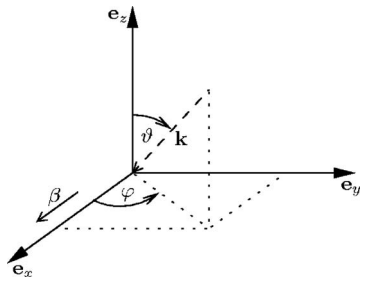

Fig. 7. Wave vector $\mathbf{k}$ of an incoming light ray in spherical coordinates $\vartheta \in (0, \pi), \varphi \in (-\pi, \pi)$ with respect to Eric's rest frame. The twin Tina is currently moving with velocity β along the $\mathbf{e}_x$ direction.

$$\mathbf{e}_1^{S'}(t') = \sinh\frac{\alpha t'}{c}\mathbf{e}_t + \cosh\frac{\alpha t'}{c}\mathbf{e}_x, \quad \mathbf{e}_3^{S'}(t') = \mathbf{e}_z. \tag{35b}$$

With the help of the local tetrad it is straightforward to derive the aberration and Doppler effect formula. Consider a wave vector $\mathbf{k}$ of an incoming light ray (compare Fig. 7). This wave vector can either be described with respect to Tina's frame $\{\mathbf{e}_i^{S'}\}_{(i=0,1,2,3)}$ or to Eric's rest frame $\{\mathbf{e}_j\}_{(j=t,x,z,y)}$. Thus,

$$\mathbf{k} = \omega(\mathbf{e}_t - \sin\vartheta\cos\varphi\mathbf{e}_x - \sin\vartheta\sin\varphi\mathbf{e}_y - \cos\vartheta\mathbf{e}_z) \tag{36a}$$

$$= \omega'(\mathbf{e}_0^{S'} - \sin\vartheta'\cos\varphi'\mathbf{e}_1^{S'} - \sin\vartheta'\sin\varphi'\mathbf{e}_2^{S'} - \cos\vartheta'\mathbf{e}_3^{S'}). \tag{36b}$$

If we transform both representations into coordinates, we can compare each component. Thus, the time component gives the Doppler shift

$$\omega = \omega'\gamma(1 - \beta\sin\vartheta'\cos\varphi'), \tag{37}$$

and from Eq. (37) we obtain the redshift factor z,

$$z = \frac{\omega}{\omega'} - 1 = \gamma(1 - \beta\sin\vartheta'\cos\varphi') - 1. \tag{38}$$

The spatial components give the aberration formulas

$$\cos\vartheta = \frac{\cos\vartheta'}{\gamma(1 - \beta\sin\vartheta'\cos\varphi')}, \tag{39a}$$

$$\cos\varphi = \frac{\sin\vartheta'\cos\varphi' - \beta}{\sin\vartheta(1 - \beta\sin\vartheta'\cos\varphi')}, \tag{39b}$$

$$\sin\varphi = \frac{\sin\vartheta'\sin\varphi'}{\gamma\sin\vartheta(1 - \beta\sin\vartheta'\cos\varphi')}. \tag{39c}$$

The inverse formulas for the Doppler shift and the aberration follow from Eqs. (37) and (39) by letting $(\beta, \omega, \vartheta, \varphi) \mapsto (-\beta, \omega', \vartheta', \varphi')$. Because aberration and the Doppler shift depend only on the relative direction, we can also use the angle χ between the wave vector $-\mathbf{k}$ and the direction of motion $\mathbf{e}_x$ with

$$\cos\chi = \sin\vartheta\cos\varphi. \tag{40}$$

From Eq. (38) it follows that Tina will see objects to be blueshifted for $z < 0$ and redshifted for $z > 0$.

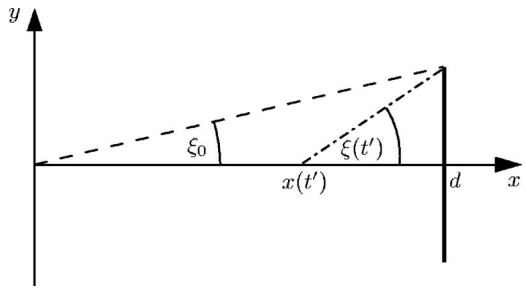

Fig. 8. An object a distance d from the origin $x=0$ has an apex angle ξ_0. An observer at rest at the current position $x(t')$ would measure an apex angle $\xi(t')$.

A similar consideration leads to length contraction. A fixed distance ℓ' to some point in the direction (ϑ',φ') with respect to Tina's current frame would have a length

$$\ell = \ell'\sqrt{\sin^2\vartheta'(\gamma^2\cos^2\varphi' + \sin^2\varphi') + \cos^2\vartheta'} \tag{41}$$

as determined by Eric.

B. Apparent size of an object

For accelerated motion objects in the direction of motion always seem to recede in the first moments even though one is approaching. The reason is also based on the aberration effect. Consider an object a distance d apart with apex angle ξ_0 as seen from the origin $x=0$, Fig. 8.

An observer at rest at the current position x given by Eq. (8) of the accelerating twin Tina would measure a current apex angle $\xi(t')$ with

$$\tan\xi(t') = \frac{d\tan\xi_0}{d - x(t')}. \tag{42}$$

The acceleration α in Eq. (8) determines whether Tina approaches $(\alpha>0)$ the object or recedes $(\alpha<0)$. The apex angle $\xi'(t')$ of the object with respect to Tina follows from the aberration formula (39b),

$$\cos\xi'(t') = \frac{1+\beta(t')\sqrt{1+\tan^2\xi(t')}}{\sqrt{1+\tan^2\xi(t')}+\beta(t')}, \tag{43}$$

where $\beta(t')$ is given by Eq. (9). Hence, from the derivative of Eq. (43) with respect to Tina's proper time t' it follows that

$$\left.\frac{d\xi'}{dt'}\right|_{t'=0} = -\frac{\alpha}{c}\sin\xi_0. \tag{44}$$

Thus, accelerating from zero velocity in the direction to the object $(\alpha>0)$ has the effect that the object initially appears to shrink, giving the impression of receding from it instead of approaching. This effect holds until $d\xi'/dt'=0$,

$$t'_n = \frac{c}{\alpha}\ln\frac{\psi_1 + \mathrm{sign}(\alpha)\delta\sqrt{(1+\tan^2\xi_0)\psi_2}}{2(1+\delta)}, \tag{45}$$

where $\delta=\alpha d/c^2$, $\psi_1=(1+\delta)^2+1+\delta^2\tan^2\xi_0$, and $\psi_2=(2+\delta)^2+\delta^2\tan^2\xi_0$.

An acceleration in the opposite direction $(\alpha<0)$ results in a magnification which has a maximum at time t'_n. Even though a velocity close to the speed of light has a tremendous magnification effect, the distance to the object grows exponentially and dominates the magnification effect.

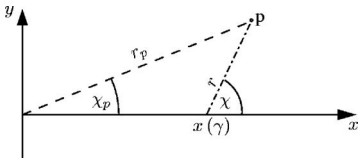

Fig. 9. An object p is located at position (r_p,χ_p) with respect to the initial position $x(\gamma=1)$ of Tina. After some time, Tina's current position is $x(\gamma)$ and the point p would have the relative position (r,χ) with respect to an observer at rest at Tina's current position.

Example. If Tina leaves home with acceleration $\alpha=-g$ away from the Sun,[13] the Sun has an apex angle $\xi_0\approx0.267°$ at a distance $d\approx1.5\times10^{11}$ m. After $t'_n\approx500$ s Tina reaches $\beta\approx1.6\times10^{-5}$, and the maximum magnification is

$$\frac{\xi'(t'_n)}{\xi_0} \approx 1 - \frac{1}{2}\frac{\alpha d}{c^2} \approx 1 + 8.2\times10^{-6}. \tag{46}$$

The angular size as seen by an observer at rest at her current distance $d(t')\approx d+1.2\times10^6$ m would be $\xi/\xi_0\approx1-8.2\times10^{-6}$.

C. Apparent position of an object

What's the apparent position of an object p with respect to the accelerating observer Tina? If we parameterize Tina's current position, Eq. (8), by her velocity, Eq. (9), we obtain

$$x = \frac{c^2}{\alpha}\{\cosh[\mathrm{arctanh}(\beta)]-1\} = \frac{c^2}{\alpha}(\gamma-1). \tag{47}$$

The position $x_p=r_p\cos\chi_p$, $y_p=r_p\sin\chi_p$ of the object p, where $r_p>0$ is the distance to the initial position of Tina and $0\leqslant\chi_p\leqslant\pi$ is the initial angle with respect to Tina's direction of motion (compare Fig. 9), transforms into Tina's frame according to the aberration formula,

$$\cos\chi' = \frac{(x_p-x)/r+\beta}{1+\beta(x_p-x)/r}, \tag{48}$$

where $r^2=(x_p-x)^2+y_p^2$.

Equation (48) can be written for $\beta\geqslant0$ as

$$\cos\chi' = \frac{[\cos\chi_p - A(\gamma-1)]/\tilde{r} + \sqrt{1-1/\gamma^2}}{1+\sqrt{1-1/\gamma^2}[\cos\chi_p - A(\gamma-1)]/\tilde{r}}, \tag{49}$$

with $A=c^2/(\alpha r_p)$ and

$$\tilde{r} = \sqrt{A^2(\gamma-1)^2 - 2A(\gamma-1)\cos\chi_p + 1}. \tag{50}$$

The observation angle $\chi'=\chi'(\beta)$ is shown in Figs. 10 and 11 for two values of A.

From the first derivative $d\chi'/d\gamma=0$ of Eq. (49) we find an extremum at

$$\gamma_e = \frac{1}{2A(A+\cos\chi_p)} + 1, \tag{51}$$

which is valid only if $(A+\cos\chi_p)>0$. The associated velocity β_e is

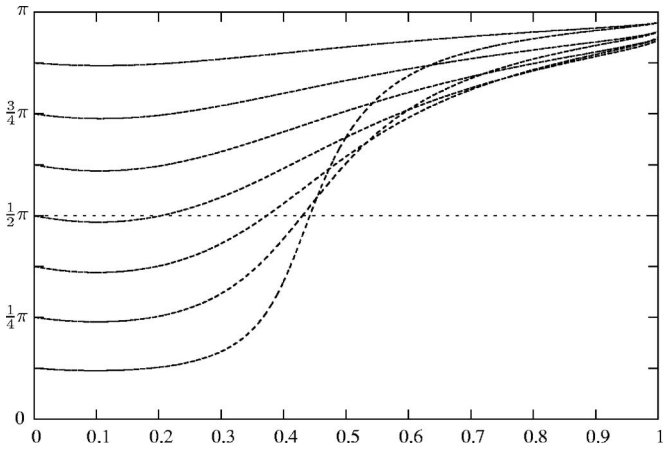

Fig. 10. The observation angle χ' is plotted versus the velocity β for $A=c^2/(\alpha r_p)\approx 9.68$. In the first instance, an object with fixed distance r_p depending on A and arbitrary angle χ_p apparently approaches the center of motion. For higher velocities, it recedes again. Because $\beta=1$ is reached only approximately, an object at (r_p,χ_p) seems to "freeze" at $\chi'_{\text{lim}}=\chi'(\beta\to 1)$.

$$\beta_e=\frac{\sqrt{1+4A\cos\chi_p+4A^2}}{1+2A\cos\chi_p+2A^2}. \tag{52}$$

For $(A+\cos\chi_p)>0$ the second derivative follows after a lengthy calculation to be

$$\left.\frac{d^2\chi'}{d\gamma^2}\right|_{\gamma_e}=\frac{\sin\chi_p}{A(\gamma_e^2-1)^2}\geqslant 0. \tag{53}$$

Thus, if there is an extremum, it is always a minimum.

In the limit $\beta\to 1$, γ goes to infinity, and an object with coordinates (r_p,χ_p) seems to "freeze" at an observation angle χ'_{lim} with respect to Tina's frame,[14]

$$\cos(\chi'_{\text{lim}})=\lim_{\gamma\to\infty}\cos\chi'=\frac{\sin^2\chi_p-A^2}{\sin^2\chi_p+A^2}. \tag{54}$$

Note that two objects p_1 and p_2 with $r_{p_1}=r_{p_2}$ and $\chi_{p_2}=\pi-\chi_{p_1}$ will "freeze" at the same observation angle χ'_{lim}.

As we have seen, the apparent position of an object depends considerably on its position (r_p,χ_p) and on the acceleration α of the observer. This dependence might be counterintuitive in some cases. From a nonrelativistic point of view, any object is located nearly behind the observer if the latter is infinitely apart from it. But in the relativistic case, the object could also appear at a different position. In brief, it is a contest between the relativistic aberration and the exponential increase of distance between star and observer.

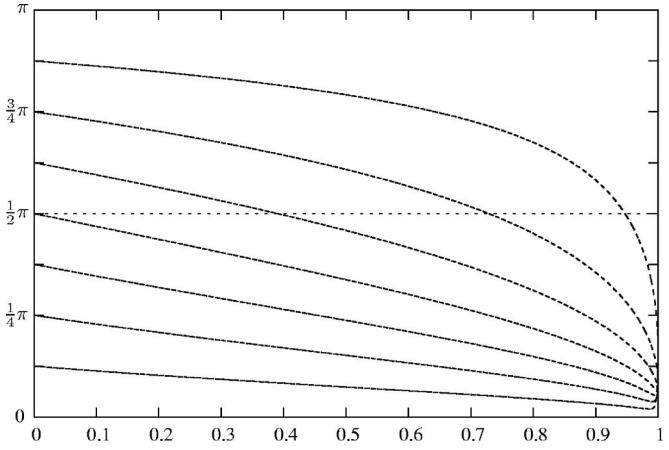

Fig. 11. The observation angle χ' is plotted versus the velocity β for $A=c^2/(\alpha r_p)\approx 0.0968$. Note that even objects that are actually behind the observer $(\chi_p>\pi/2)$ might apparently "freeze" in front of the observer.

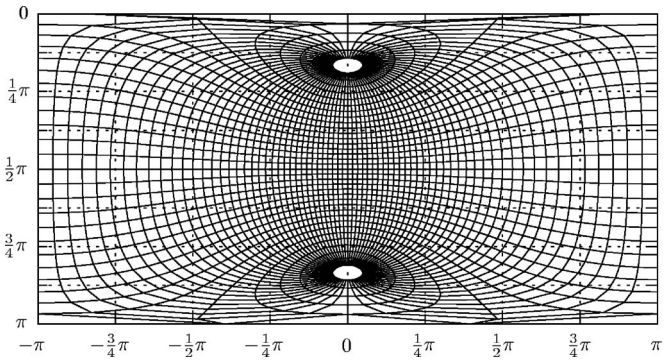

Fig. 12. Stellar sky at $\beta=0.5$ in the 4π-representation where $\varphi=(-\pi,\pi)$ is the abscissa and $\vartheta=(0,\pi/2)$ is the ordinate. The center of the image $(\vartheta=\pi/2,\varphi=0)$ corresponds to the direction of motion. The circles of latitude and the meridians are separated by 5°.

VII. VISUALIZATION OF THE STELLAR SKY

A. Aberration and Doppler shift

What could Tina really see if she looked through a window of her rocket? If there were a sphere fixed at infinity with circles of latitude and meridians each separated by 5°, Tina would see a warped lattice as in Figs. 12 and 13. In contrast to the visualization of Scott and van Driel[15] we use the 4π representation where the azimuth angle φ and the zenith distance ϑ are plotted like Cartesian coordinates to show the full sky. The disadvantage of this representation is the distortion at the nodes $\vartheta=0$ and $\vartheta=\pi$. Here, the direction of motion corresponds to the center of the representation $(\vartheta=\pi/2,\varphi=0)$.

Because of aberration, Eq. (39) shows that the nodes of the stellar sphere move together according to Tina's velocity. Their angular separation $\Delta\vartheta'$ follows from Eq. (39a),

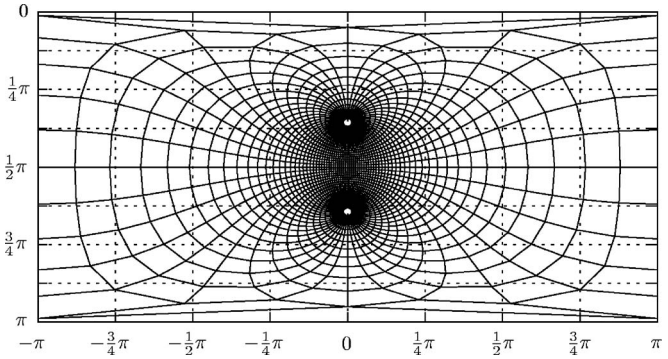

Fig. 13. Stellar sky at $\beta=0.9$ in the 4π representation. Because of aberration, the nodes of the stellar sphere move together.

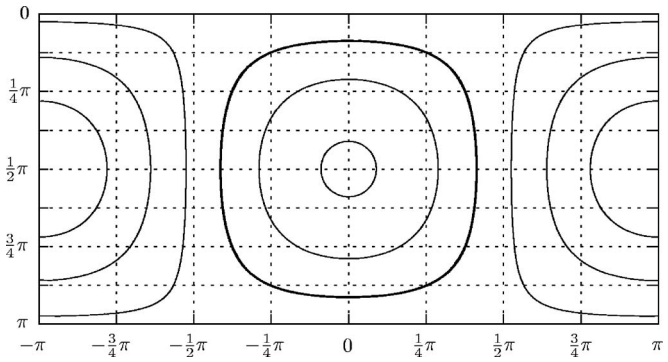

Fig. 14. Lines of constant redshift z at velocity β=0.5 in the 4π representation. From inside to outside: z=−0.4 to z=0.6, step 0.2; the bold line marks z=0.

$$\Delta\vartheta' = \pi - 2\arccos\sqrt{1-\beta^2}. \tag{55}$$

Because angular distance becomes smaller in the direction of motion, an object seems to be farther away in comparison to its real distance. In contrast, objects in the opposite direction seem to grow.

Besides the mere geometrical aspects, Figs. 14 and 15 show lines of constant Doppler shift at different velocities. As long as the velocity β=0, there is no Doppler shift, but for $\beta>0$ light is Doppler shifted following Eq. (38),

$$z = \gamma(1-\beta\cos\chi') - 1, \tag{56}$$

where χ' is the angle between the direction of motion and the incoming light ray.

Zero Doppler shift occurs for $\beta>0$ at an angle χ'_0 with

$$\cos\chi'_0 = \frac{1-\sqrt{1-\beta^2}}{\beta}. \tag{57}$$

The difference Δz between the maximum blueshift and the maximum redshift equals

$$\Delta z = z(\chi'=\pi) - z(\chi'=0) = 2\beta\gamma. \tag{58}$$

Thus, the faster Tina moves, the more of the sky is redshifted. Only a small portion of the sky in the direction of motion is blueshifted.

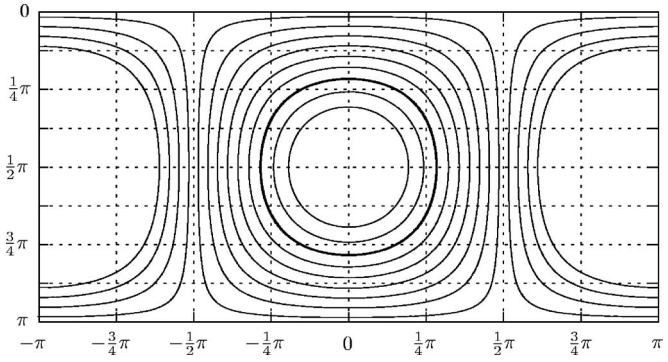

Fig. 15. Lines of constant redshift z at velocity β=0.9 in the 4π representation. From inside to outside: z=−0.4 to z=2.0, step 0.2; the bold line marks z=0. Note that most of the sky is redshifted even for directions $\chi' < \pi/2$.

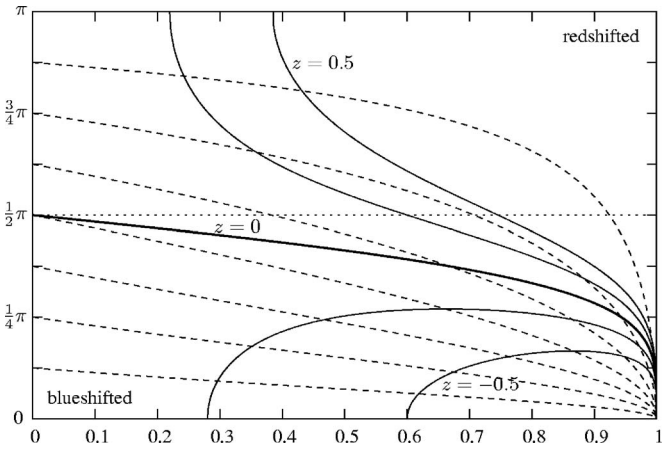

Fig. 16. The observation angle χ' is plotted versus the velocity β. The solid lines are lines of constant Doppler shift z according to Eq. (59); the dashed lines represent the aberration of the angle χ (see Eq. (60)).

Another interesting detail is shown in Fig. 16, where the observed angle χ' is plotted versus the velocity β according to the Doppler shift,

$$\chi' = \arccos\left(\frac{1-(z+1)\sqrt{1-\beta^2}}{\beta}\right), \tag{59}$$

and aberration

$$\chi' = \arccos\left(\frac{\cos\chi+\beta}{1+\beta\cos\chi}\right). \tag{60}$$

For β=0 there is no Doppler shift and no aberration.

Objects in front of the observer, $\chi<\pi/2$, will always be blueshifted and seem to be in front of the observer, $\chi'<\pi/2$. But, for objects in back of the observer, $\chi>\pi/2$, whether they apparently are in front or not depends on the velocity. An object at an angle $\chi>\pi/2$ will turn from being redshifted to being blueshifted when β is greater than

$$\beta_{\text{red-blue}} = -\frac{2\cos\chi}{1+\cos^2\chi}. \tag{61}$$

B. Temperature and brightness

For visualizing the stellar sky we use the Hipparcos star catalogue.[16] We extract the Johnson B-V color and assign a temperature $T=T_{\text{B-V}}$ to each star by the empirical law[17]

$$B-V = \begin{cases} C_1\log_{10}(T)+C_2 & (\log_{10}T \leqslant 3.961) \\ C_3\log_{10}(T)^2 + C_4\log_{10}(T) + C_5 & (\log_{10}T > 3.961) \end{cases} \tag{62}$$

with constants from Table I. Equation (62) is only a limited approximation to the real temperatures of the stars, but it simplifies the following calculations.

We also need the bolometric correction (BC)[18] to transform from the visual M_V to the bolometric magnitude M_{bol},

$$M_{\text{bol}} = M_V + BC, \tag{63}$$

with

$$BC = C_6\tilde{t}^4 + C_7\tilde{t}^3 + C_8\tilde{t}^2 + C_9\tilde{t} + C_{10}, \tag{64}$$

where $\tilde{t}=\log_{10}(T)-4$.

Table I. The coefficients C_i for Eqs. (62) and (64) are taken from Ref. 17.

Coefficient	Value	Coefficient	Value
C_1	−3.684	C_6	−8.499
C_2	14.551	C_7	13.421
C_3	0.344	C_8	−8.131
C_4	−3.402	C_9	−3.901
C_5	8.037	C_{10}	−0.438

Instead of the actual spectrum of each star we use a Planck spectrum at temperature $T=T_{B-V}$ with spectral intensity

$$I_\nu = \frac{2h\nu^3}{c^2}\frac{1}{e^{h\nu/(k_B T)}-1}, \tag{65}$$

where h is Planck's constant and k_B is Boltzmann's constant.[20] If the spectral intensity is expressed in terms of wavelength, we obtain from $I_\nu d\nu = -I_\lambda d\lambda$ and $c=\lambda\nu$ the expression

$$I_\lambda = \frac{2hc^2}{\lambda^5}\frac{1}{e^{hc/(\lambda k_B T)}-1}. \tag{66}$$

The typical shape of a Planck spectrum is shown in Fig. 17, where the wavelength $\lambda_{\max}$ of the maximum of the intensity follows from Wien's displacement law

$$\lambda_{\max} T = b, \tag{67}$$

with Wien's displacement constant $b=2.8978\times10^{-3}$ km.

We use a Planck spectrum here, because it simply transforms with the Doppler factor according to the relativistic Liouville theorem.[21] From $I_\nu/\nu^3=$constant together with Eqs. (65) and (38) the temperature transforms as

$$\frac{T_{\text{star}}}{T'_{\text{star}}} = \frac{\nu}{\nu'} = z+1. \tag{68}$$

Thus, a blueshifted star with $-1<z<0$ seems to be hotter than it really is compared to its own rest frame.

The luminosity L of an isotropically radiating black body of radius R is given by $L=4\pi\sigma R^2 T^4$ with the Stefan–Boltzmann constant $\sigma\approx5.67\times10^{-8}$ Wm^{-2} K^{-4}.[19] Thus, the absolute bolometric magnitude M_{bol} of an object with a Planck spectrum at temperature T is

$$M_{\text{bol}} - M_{\text{bol},\odot} = -2.5\log_{10}\frac{L}{L_\odot} = -5\log_{10}\frac{R}{R_\odot} - 10\log_{10}\frac{T}{T_\odot}, \tag{69}$$

where we approximated the spectrum of the sun by a Planck spectrum at temperature $T_\odot$.[22] Because the absolute bolometric magnitude M_{bol} is defined as the brightness of a star at a distance of 10 pc, the apparent bolometric magnitude m_{bol} is given by

$$m_{\text{bol}} - M_{\text{bol}} = 5\log_{10}\frac{r}{10\text{pc}}, \tag{70}$$

where r is the distance between the star and the observer.[19]

From Tina's point of view, we have to transform the Planck spectrum of a star into her current rest frame according to Eq. (68) resulting in a different absolute bolometric magnitude M'_{bol},

$$M'_{\text{bol}} - M_{\text{bol},\odot} = -5\log_{10}\frac{R'}{R_\odot} - 10\log_{10}\frac{T'}{T_\odot}. \tag{71}$$

If we subtract Eq. (69) from Eq. (71), the transformation between the absolute bolometric magnitudes reads

$$M'_{\text{bol}} - M_{\text{bol}} = -5\log_{10}\frac{R'}{R} - 10\log_{10}(z+1), \tag{72}$$

where we have used Eq. (68) for the transformation of the temperatures. Because we are interested in the apparent magnitudes, we substitute the absolute magnitudes by means of Eq. (70),

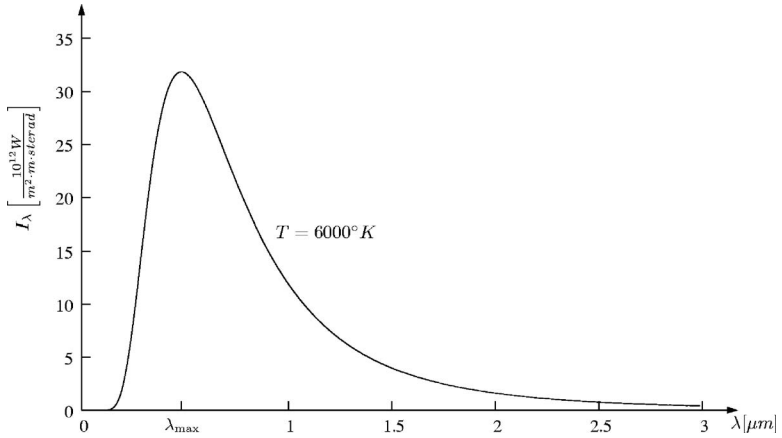

Fig. 17. Planck spectrum at temperature $T=6000$ K with a maximum at $\lambda_{\max}\approx0.483$ μm.

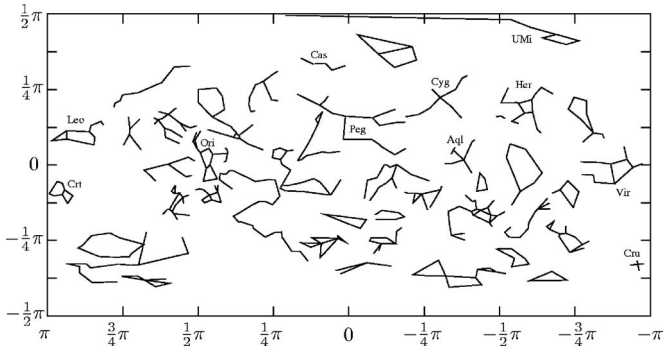

Fig. 18. The stellar sky marked by some constellations as seen at rest. In the 4π representation the right ascension α is plotted on the abscissa and the declination δ is plotted on the ordinate. Abbreviations: (Aql) Aquila, (Cas) Cassiopeia, (Crt) Crater, (Cru) Crux, (Cyg) Cygnus, (Her) Hercules, (Leo) Leo, (Ori) Orion, (Peg) Pegasus, (UMi) Ursa Minor.

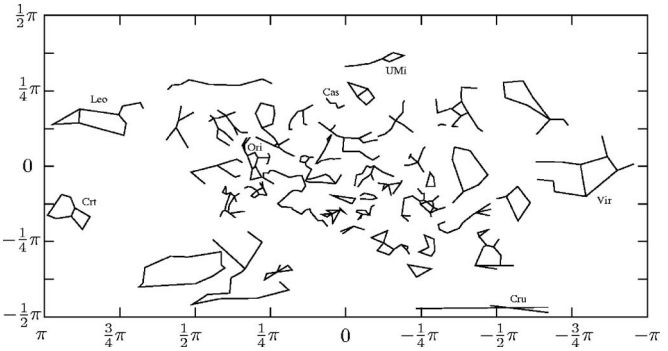

Fig. 19. The stellar sky as seen by an observer passing the Earth with 50% of the speed of light. The distortion of the constellation Southern Cross (Cru) is due to the 4π projection and the aberration effect (see Fig. 12).

$$m'_{\mathrm{bol}} - m_{\mathrm{bol}} = -5\log_{10}\frac{rR'}{r'R} + 10\log_{10}(z+1). \tag{73}$$

As long as we approximate the stars as nearly point-like sources which are very far from Tina's current position, we can write $\Delta\chi = 2R/r$, where $\Delta\chi$ is the angular diameter of the star. With the apparent angular diameter $\Delta\chi'$ as seen from Tina's reference frame, we obtain

$$m'_{\mathrm{bol}} - m_{\mathrm{bol}} = -5\log_{10}\frac{\Delta\chi'}{\Delta\chi} + 10\log_{10}(z+1). \tag{74}$$

Here, the quotient $\Delta\chi'/\Delta\chi$ can be replaced by the derivative of the aberration formula (60),

$$\frac{d\chi'}{d\chi} = \frac{1}{\gamma(1+\beta\cos\chi)}. \tag{75}$$

As expected, the transformation of the apparent magnitude, Eq. (74), is composed of an aberration and a Doppler shift component.

If we cannot approximate the stars to be nearly point-like, we have to take their expansion into account. For more information on what an expanded star would look like, we refer the reader to Ref. 23. Because we cannot extract the size of a star from the Hipparcos catalogue, we neglect its expansion.

C. Constellations

We have discussed how aberration and Doppler shift determine the view of the stellar sky as seen by a relativistic observer. Figures 18–20 show the stellar sky of an observer from the position of the Earth but at different velocities in the direction right ascension $\alpha=0$ and declination $\delta=0$. Note that the declination δ corresponds to $\pi/2-\vartheta$ in comparison to Fig. 7. The stars are connected by lines showing the constellations.[24]

As explained in Sec. VI B, the aberration effect lets the constellations apparently shrink in the direction of motion, while the ones that are behind the observer, such as Leo, Virgo (Vir) and Crater (Crt), seem to grow.

In Table II we list the stars of the constellations Orion (Ori), Cassiopeia (Cas), and Southern Cross (Cru) with their rest frame data. For these constellations we give in Tables III and IV the apparent distance d', the temperature T', and the bolometric magnitudes m_{bol} for $\beta=0.5$ and $\beta=0.9$. The apparent distance d' follows from the inverse form of Eq. (41),

$$d' = d\left[\gamma^2 - \beta^2\frac{1-\cos^2\delta\cos^2\alpha}{(1+\beta\cos\delta\cos\alpha)^2}\right]^{-1/2}, \tag{76}$$

where the distance d, measured in parsec, is related to the trigonometric parallax π via $d=1/\pi$. The redshift factor z is given by the inverse of Eq. (37),

$$z = \frac{\omega}{\omega'} - 1 = \frac{1}{\gamma(1+\beta\cos\delta\cos\alpha)} - 1, \tag{77}$$

and determines the temperature $T'=T/(z+1)$.

Because Cassiopeia and Orion are in front of the observer, $\chi_{\mathrm{Cas}}\approx 1.07$ and $\chi_{\mathrm{Ori}}\approx 1.47$, they will always be blueshifted (see Fig. 16). But the Southern Cross (Cru), $\chi_{\mathrm{Cru}}\approx 2.14$, will be redshifted until the observer reaches the velocity $\beta_{\text{red-blue}}\approx 0.83$, which follows from Eq. (61). At $\beta=\beta_{\text{red-blue}}$ Cru has apparently already changed from the back side to the front side of the observer. This change follows from Eq. (60) and occurs at

$$\beta_{\chi'=\pi/2} = -\cos\chi_{\mathrm{Cru}} \approx 0.53. \tag{78}$$

We have written the interactive Java applet `RelSkyApplet`[11] for visualizing the stellar sky at different velocities as seen from the position of the Earth. The applet clearly demonstrates the strong geometrical distortion as well as the direction dependent Doppler shift for velocities closed to the speed of light. A short introduction is given in

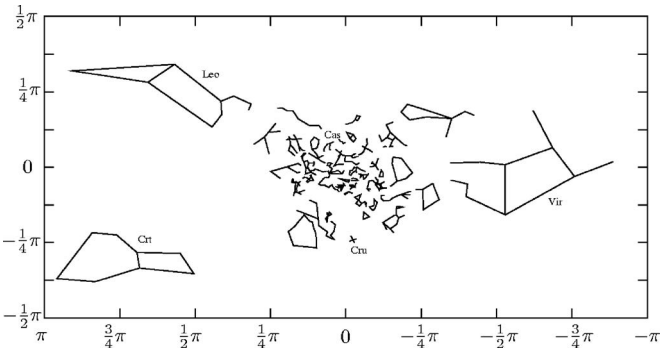

Fig. 20. The stellar sky as seen by an observer passing the Earth with 90% of the speed of light.

Table II. Star data of some constellations from Figs. 18–20. α: right ascension, δ: declination, π: trigonometric parallax (milliarcsec), B-V: Johnson B-V color, T: temperature (Kelvin) from Eq. (62), HIP: Hipparcos number.

Abbr.	α	δ	π	B-V	T	HIP
α Ori	1.5497	0.1293	7.63	1.50	3488	27989
β Ori	1.3724	−0.1431	4.22	−0.03	9077	24436
γ Ori	1.4187	0.1108	13.42	−0.22	19245	25336
δ Ori	1.4487	0.0052	3.56	−0.17	15279	25930
ϵ Ori	1.4670	−0.0210	2.43	−0.18	15903	26311
ζ Ori	1.4868	−0.0339	3.99	−0.20	17038	26727
κ Ori	1.5174	−0.1688	4.52	−0.17	14819	27366
α Cas	0.1767	0.9868	14.27	1.17	4287	3179
β Cas	0.0400	1.0324	59.89	0.38	7025	746
γ Cas	0.2474	1.0597	5.32	−0.05	9295	4427
δ Cas	0.3744	1.0513	32.81	0.16	8060	6686
ϵ Cas	0.4991	1.1113	7.38	−0.15	13732	8886
α Cru	−3.0255	−1.1013	10.17	−0.24	21259	60718
β Cru	−2.9334	−1.0418	9.25	−0.24	20696	62434
γ Cru	−3.0056	−0.9968	37.09	1.60	3277	61084
δ Cru	−3.0755	−1.0254	8.96	−0.19	16569	59747

Appendix A while a more detailed discussion as well as several examples can be found in the help menu of the applet.

VIII. A TRIP TO THE END OF THE UNIVERSE

As a first trip Tina goes on an expedition to the center of our galaxy (SgrA*) 8 kpc away. From Table V we see that her maximum speed is only 2.8 ppb (parts per billion) below the speed of light.

With this tremendous velocity even the extremely cold microwave background radiation[25] at $T_{\text{cmb}}=2.725$ K comes into the visual regime. But in contrast to one's expectation, the Doppler shifted background radiation will not fill the whole sky. By Wien's displacement law (67) an object must have a temperature of about $T_{780}\approx 3700$ K to emit its maximum radiation in the red light regime with $\lambda=780$ nm. To shift the background temperature to T_{780} the observer has to move with a velocity very close to the speed of light, $\beta_{780}\approx 1-1.07\times 10^{-6}$. From Eq. (57) it follows that the background radiation is blueshifted only in the small region of $\chi_0'<3°$. The rest of the sky is redshifted with maximum $z\approx 1767$ at $\chi'=\pi$.

In contrast, the redshift brings the x-ray and γ-ray sky down to the visual regime. For x rays with wavelengths of $\lambda\approx 10^{-10}$ m Tina has to fly with $\beta\gtrapprox 1-6.6\times 10^{-7}$. The much higher velocity $\beta\gtrapprox 1-6.6\times 10^{-12}$ is needed for γ rays with $\lambda\approx 10^{-12}$ m.[26] Just before the γ-ray sky, the hydrogen 21 cm

Table III. The stars of Table II have distance d' (parsec) and temperature T' (Kelvin) at velocities $\beta=0.5$ and $\beta=0.9$ in the direction $\alpha=\delta=0$.

Abbr.	$d_{\beta=0}$	$d'_{\beta=0.5}$	$T'_{\beta=0.5}$	$d'_{\beta=0.9}$	$T'_{\beta=0.9}$
α Ori	131.06	125.61	4070	61.90	8153
β Ori	236.97	222.56	11503	109.31	24479
γ Ori	74.52	70.35	23895	34.56	50135
δ Ori	280.90	266.08	18717	130.76	38894
ϵ Ori	411.52	390.64	19315	192.02	39886
ζ Ori	250.63	238.46	20499	117.27	42038
κ Ori	221.24	211.27	17562	103.98	35608
α Cas	70.08	63.34	6294	31.32	14641
β Cas	16.70	15.13	10190	7.48	23547
γ Cas	187.97	171.11	13277	84.45	30424
δ Cas	30.48	27.78	11457	13.71	26181
ϵ Cas	135.50	14.49	18943	61.30	42544
α Cru	98.33	98.26	19032	53.01	29046
β Cru	108.11	108.11	17998	59.70	26380
γ Cru	26.96	26.95	2766	15.31	3878
δ Cru	111.61	111.60	14181	62.54	20304

Table IV. The apparent visual magnitude m_V of the stars of Table II have bolometric magnitudes m_{bol}^{β} at velocities $\beta=0$, $\beta=0.5$, and $\beta=0.9$ in the direction $\alpha=\delta=0$.

Abbr.	m_V	BC	$m_{\text{bol}}^{\beta=0}$	$m_{\text{bol}}^{\beta=0.5}$	$m_{\text{bol}}^{\beta=0.9}$
α Ori	0.45	−2.01	−1.56	−2.32	−6.88
β Ori	0.18	−0.29	−0.11	−1.27	−6.10
γ Ori	1.64	−1.95	−0.31	−1.38	−6.14
δ Ori	2.25	−1.36	0.89	−0.11	−4.83
ϵ Ori	1.69	−1.46	0.23	−0.73	−5.42
ζ Ori	1.74	−1.63	0.11	−0.81	−5.47
κ Ori	2.07	−1.28	0.79	−0.05	−4.66
α Cas	2.24	−0.93	1.31	−0.57	−5.77
β Cas	2.28	−0.08	2.20	0.37	−4.80
γ Cas	2.15	−0.32	1.83	0.07	−5.06
δ Cas	2.66	−0.16	2.50	0.78	−4.35
ϵ Cas	3.35	−1.10	2.25	0.67	−4.38
α Cru	0.77	−2.21	−1.44	−0.97	−4.14
β Cru	1.25	−2.14	−0.89	−0.29	−3.24
γ Cru	1.59	−2.45	−0.86	−0.13	−2.82
δ Cru	2.79	−1.56	1.23	1.90	−0.91

Table V. Distance from Earth, maximum speed and proper time of both twins for several stellar destinations. In the solar system we will reach only a few percent of the speed of light. Thus, time dilation can be neglected. However, in the neighborhood of the solar system time dilation is crucial. The "END" of the universe represents the maximum distance of about 13.7 billion light years that astronomers are able to observe.

Object	Distance	$\beta_{max}=v_{max}/c$	Tina's time $2T'$	Eric's time $2T$
Mars	0.524 AU≈4.4 lm	0.003	$49^{h}45^{min}13.4^{sec}$	$49^{h}45^{min}13.7^{sec}$
Saturn	8.53 AU≈1.2 lh	0.012	$8^{d}8^{h}44^{min}21^{sec}$	$8^{d}8^{h}44^{min}38^{sec}$
Pluto	38.81 AU≈5.4 lh	0.025	$17^{d}20^{h}10^{min}$	$17^{d}20^{h}13^{min}$
α Cen C (HIP 70890)	1.29 pc	0.949	3.54[a]	5.84[a]
Vega (HIP 91262)	7.76 pc	0.9975	6.46[a]	27.17[a]
SgrA*	8 kpc	$1-2.8\times10^{-9}$	19.74[a]	26[ka]
LMC	50 kpc	$1-7.1\times10^{-11}$	23.30[a]	163[ka]
M81	2 Mpc	$1-4.4\times10^{-14}$	30.45[a]	6.5[Ma]
END	13.7×10^{9} ly	$1-1.0\times10^{-20}$	45.27[a]	13.7[Ga]

line of interstellar gas, resulting from a transition between two hyperfine structure energy levels in the hydrogen atom, will become visible at a velocity of $\beta\approx1-2.7\times10^{-11}$.

A wavelength λ will be seen at wavelength λ' for a velocity

$$\beta=\left|\frac{\lambda'^2-\lambda^2}{\lambda'^2+\lambda^2}\right|. \tag{79}$$

Thus, the minimum and maximum wavelengths at velocity β that are transformed into the visual regime follow from

$$\lambda_{min}=380\text{ nm}\sqrt{\frac{1-\beta}{1+\beta}}\quad\text{and}\quad\lambda_{max}=780\text{ nm}\sqrt{\frac{1+\beta}{1-\beta}}.$$

What happens with the Milky Way in the meantime? While Tina's journey to the center of our galaxy lasts only 20 years with respect to her proper time, the Milky Way ages about 26,000 years. In that time, our sun with rotational velocity[27] $v\approx220$ km/s$\approx7.34\times10^{-4}$ ly/y (light years per year) will cover a distance of about 19 ly. To fully describe the galactic evolution, we need the position as well as the proper motion of each star in the galaxy. The Hipparcos catalogue, which consists of about 118,000 stars, with most of them at a distance of about 100 pc, delivers the best positional star reference (1 milli-arc-sec). From the GAIA[29] mission we expect an accuracy in positional astrometry of about 20 μas. Thus, all stars in our galaxy up to the 20th magnitude should be included.

As in the title of this article, Tina could also go on a trip to the "end of the universe" within her lifetime. Here, the "end" means the maximum distance of about 13.7 billion light years that astronomers are able to observe. For these speculations we neglect the expansion of the universe, but do the calculations in the flat Minkowskian spacetime instead of a Robertson–Walker[5] spacetime.

When Tina reaches her maximum velocity $\beta=1-\epsilon$ with $\epsilon=1.0\times10^{-20}$ in the middle of her journey, the relativistic effects are extremely dramatic. A γ factor of about 7.07×10^{9} results in a different time rate: $\Delta t'=1$ s corresponds to $\Delta t=224a$! Thus, in roughly 12 days with respect to Tina's proper time our Sun would have finished one revolution around the center of our galaxy. Zero Doppler shift occurs at an angle $\chi_0'\approx\sqrt[4]{8\epsilon}\approx3.5$ as. The maximum blueshift in the direction of motion is $z(\chi'=0)\approx\sqrt{\epsilon/2}\approx-1+7.07\times10^{-11}$, whereas the maximum redshift is $z(\chi'=\pi)\approx\sqrt{2/\epsilon}\approx1.4\times10^{10}$. Because the transition from redshift to blueshift is quite strong, Tina would see only a very small, bright dot in the direction of motion. In contrast, most of the sky would be very cold and very dark. Navigation by stars would be completely impossible.

One might ask if she would be able to see the evolution of the universe.[37]

ACKNOWLEDGMENTS

The authors thank Professor Hanns Ruder for the idea of this work and Professor Jörg Frauendiener for many discussions and for carefully reading the manuscript. Thanks also to Professor Jeff Rabin for the suggestion of the book *Tau Zero* (see Ref. 30). This work was supported by the Deutsche Forschungsgesellschaft (DFG), SFB 382, Teilprojekt D4.

APPENDIX A: JAVA APPLETS

The Java applets used to generate the diagrams in this article are available from the Electronic Physics Auxiliary Publication Service (EPAPS).[11] The Java applet `TwinApplet` generates the diagrams of Sec. V. There are three input parameters, two of them are obligatory: the acceleration of the traveling twin Tina in terms of Earth's gravity g and either her travel time or the maximum reachable distance. With these parameters four plots are generated. They are grouped in two panels: one showing the distance and the velocity of Tina and the other showing the time signals which the twins receive of each other.

The acceleration of Tina can be modified between 10^{-6} g and 10^{3} g. The travel time of one acceleration phase can be entered either into a text field or with a slider. While moving the time slider, we can observe the immediate change of the plots and the maximum reachable distance. The maximum time is limited to the time that the twin needs to reach the end of the universe. Alternatively we can choose the travel distance and hence calculate the time needed. It is possible to save the plots as PNG images or the calculated data points in a text file.

Because we have to deal with velocities very close to the speed of light, the usual double-precision floating-point numbers will not suffice, compare Appendix B. Thus, we use a series expansion for the equations depending on the velocity β.

The Java applet `RelSkyApplet` can visualize either the stellar sky, the star constellations, or the cosmic microwave background, each with different velocities as seen by an ob-

server passing the Earth. The main input parameters for all the views are the velocity and the line of sight (right ascension and declination). For the stellar sky there are some additional parameters such as the maximum displayed magnitude and the magnitude scale. For the stellar sky and the star constellations it is possible to increase the velocity stepwise (without changing position) to observe the increase of aberration and Doppler shift. By varying the velocity, the user obtains a better understanding of how relativistic aberration and the Doppler shift affects the visualization.

It is possible to choose between two views for the visualizations: a 4π-representation or an hemispherical representation. In both cases the line of sight corresponds to the center of the representation and can be set manually. The stellar sky can also be seen from any desired point in our galaxy (either in equatorial coordinates or in galactic coordinates). By moving the mouse over the sky view, the sky coordinates of the actual mouse position are displayed in the lower left corner of the applet. The longitude and latitude of the sky can also be displayed as a grid, which deforms according to the increasing velocity.

The stars are realized as small disks whose colors are calculated according to Appendix C and the star temperatures. It is possible to change the color mode in order to examine a particular temperature range. In manual mode the colors that are displayed correspond to an arbitrary color scale. The size of the disk represents the star's apparent bolometric magnitude m_{bol}.

By clicking on a star its Hipparcos identifier and its common name (if available) are displayed. A click on `Get Info` provides further information about the star: the complete Hipparcos data set, and some of its real values compared to its apparent values.

The star constellations view is suitable for observing the distortion due to the aberration effect. Remember that the distortion of some constellations in the border area of the 4π-representation might be caused by the representation itself.

The basic data of the cosmic microwave background was obtained from the Wilkinson Microwave Anisotropy Probe (WMAP).[31] To speed up the applets' execution, the original data was downgraded to a 4π representation with an image resolution of 720×360 pixels. By selecting the microwave mode the color scale is automatically set to a temperature range of 2.5–2.9 K (which corresponds to microwave wavelengths). Due to the Doppler effect, it is also possible to observe the microwave background even in the visual regime (visual color mode) starting at a velocity of about $0.999c$.

APPENDIX B: NUMERICAL CALCULATIONS

As we can see from Table V, we have to consider velocities β that are very close to the speed of light. But computers can handle only a limited number of digits. In general, double-precision floating-point numbers with a 52 bit mantissa are used for precise calculations.[32] For clarity we will describe here the velocity $\beta=1-10^{-5}$ as a single-precision floating-point number with a 23 bit mantissa

$$\hat{\beta}=1.11111111111111101011000_2\times2^{-1}\approx0.9999899864_{10}, \tag{B1}$$

where $\hat{\beta}$ is expressed either in normalized binary form (subscript 2) or in decimal form (subscript 10). This machine

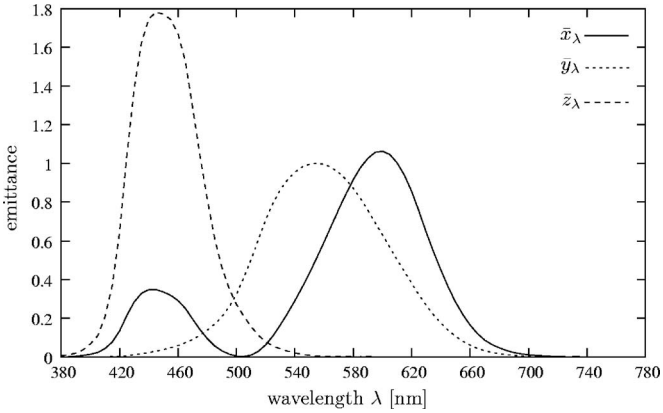

Fig. 21. CIE 1931 2-deg color matching functions $\bar{x}_\lambda,\bar{y}_\lambda,\bar{z}_\lambda$.

impreciseness propagates. Hence, a straightforward numerical calculation of the γ-factor results in

$$\hat{\gamma}=1.10111110111010010000011_2\times2^7\approx223.455123_{10}. \tag{B2}$$

The series expansion of the γ factor is

$$\gamma=\frac{1}{\sqrt{1-(1-\varepsilon)^2}}\approx\frac{1}{\sqrt{2\varepsilon}}+\mathcal{O}(\varepsilon^{1/2}), \tag{B3}$$

and the evaluation of $\varepsilon=10^{-5}$ gives

$$\hat{\gamma}=1.10111111001101101010111_2\times2^7\approx223.606796_{10}. \tag{B4}$$

From the relative errors E^{rel} for the straightforward calculation and the series expansion,

$$E^{\mathrm{rel}}_{\mathrm{straight}}\approx6.8\times10^{-4}\quad\text{and}\quad E^{\mathrm{rel}}_{\mathrm{series}}\approx2.5\times10^{-6}, \tag{B5}$$

we conclude that it is important to replace an equation by its series expansion for high velocities.

APPENDIX C: FROM SPECTRUM TO COLOR

The human visual perception of wavelengths lies in the range between 380 and 780 nm. There are three types of cones in the retina which are sensitive to red, green and blue light. Hence, any visible color can be composed of three primary colors.[33]

In 1931 the Commission Internationale de l'Éclairage (CIE) defined three primary colors **X**, **Y**, and **Z** with the corresponding color matching functions[34] $\bar{x}(\lambda)$, $\bar{y}(\lambda)$ and $\bar{z}(\lambda)$ (see Fig. 21).

Any color $\mathbf{C}=X\mathbf{X}+Y\mathbf{Y}+Z\mathbf{Z}$ can be composed of these primary colors,[35] where the components X, Y and Z follow from the spectral intensity distribution $I(\lambda)$ by convolution with the color matching functions, for example,

$$X=k\int I(\lambda)\bar{x}(\lambda)d\lambda. \tag{C1}$$

Because we are interested only in the chromaticity values x, y, and z with $x=X/(X+Y+Z)$ and $y=Y/(X+Y+Z)$ and $z=1-x-y$, the constant k cancels out. To find the RGB values for a specific device, we need its primary chromaticity values $x_{(r,g,b,w)}$ and $y_{(r,g,b,w)}$ for red, green, blue and the white

point.[36] After the transformation from xyz to rgb, we normalize the rgb values according to their maximum,

$$(r,g,b) \mapsto \frac{(r,g,b)}{\max(r,g,b)}, \tag{C2}$$

which has the effect that all colors have their largest possible brightness.

[a]Author to whom correspondence should be addressed. Electronic mail: tmueller@tat.physik.uni-tuebingen.de

[1]R. D'Inverno, *Introducing Einstein's Relativity* (Clarendon Press, Oxford, 1992).
[2]C. E. Dolby and S. F. Gull, "On radar time and the twin 'paradox,'" Am. J. Phys. **69**, 1257–1261 (2001).
[3]S. P. Boughn, "The case of the identically accelerated twins," Am. J. Phys. **57**, 791–793 (1988).
[4]R. P. Gruber and Richard H. Price, "Zero time dilation in an accelerating rocket," Am. J. Phys. **65**, 979–980 (1997).
[5]W. Rindler, *Relativity: Special, General, and Cosmology* (Oxford University Press, New York, 2001).
[6]R. U. Sexl, and H. K. Urbantke, *Relativity, Groups, Particles: Special Relativity and Relativistic Symmetry in Field and Particle Physics* (Springer, Wien/New York, 2000).
[7]R. Perrin, "Twin paradox: A complete treatment from the point of view of each twin," Am. J. Phys. **47**, 317–319 (1979).
[8]A. P. French, *Special Relativity* (W. W. Nelson & Co, London, 1968).
[9]R. H. Good, "Uniformly accelerated reference frame and twin paradox," Am. J. Phys. **50**, 232–238 (1982).
[10]H. und M. Ruder, *Die Spezielle Relativitätstheorie* (Vieweg Studium, Braunschweig/Wiesbaden, 1993).
[11]See EPAPS Document No. E-AJPIAS-76-002803 for the Java applets, `RelSkyApplet` and `TwinApplet`, and accompanying help manuals. This document can be reached through a direct link in the online article's HTML reference section or via the EPAPS homepage (http://www.aip.org/pubservs/epaps.html).
[12]One light year (1 ly) equals the distance which is covered by light with velocity $c=299,792,458$ m/s in one year.
[13]The negative acceleration of Tina away from the Sun equals the situation where Tina has positive acceleration but looks contrary to her direction of motion.
[14]The limit can be calculated using l'Hospital's rule.
[15]G. D. Scott and H. J. van Driel, "Geometrical appearances at relativistic speeds," Am. J. Phys. **38**, 971–977 (1970).
[16]The Hipparcos star catalogue consists of about 118,000 stars most of which are at a distance of roughly 100 pc. The data we are interested in are right ascension (H3), declination (H4), magnitude in Johnson V (H5), trigonometric parallax (H11), Johnson B-V color (H37), and Henry Draper (HD) catalogue number (H71). The digital catalogue I/239 can be found at ⟨cdsarc.u-strasbg.fr/viz-bin/Cat?I/239⟩ 1997HIP…C……0E-European Space Agency SP-1200.
[17]B. C. Reed, "The composite observational-theoretical HR diagram," J. R. Astron. Soc. Can. **92**, 36–37 (1998).
[18]The bolometric magnitude of a star is defined by the flux density integrated over all wavelengths. However, a real telescope can only measure the flux density within a small region of wavelengths. The bolometric correction compensates the difference between the bolometric and the visual magnitude (Ref. 19).
[19]*Fundamental Astronomy*, edited by Hannu Karttunen, Pekka Kröger, Heikki Oja, Markku Poutanen, and Karl J. Donner (Springer-Verlag, Heidelberg, 2003).
[20]We take the physical constants from the National Institute of Standards and Technology, ⟨physics.nist.gov/cuu/Constants⟩.
[21]R. W. Lindquist, "Relativistic transport theory," Ann. Phys. **37**, 487–518 (1966).
[22]The absolute bolometric magnitude of the sun is $M_{\mathrm{bol},\odot}=4.83$ and the effective temperature is $T_\odot \approx 5778$ K, see also ⟨nssdc.gsfc.nasa.gov/planetary/factsheet/sunfact.html⟩.
[23]U. Kraus, "Brightness and color of rapidly moving objects: The visual appearance of a large sphere revisited," Am. J. Phys. **68**, 56–60 (2000).
[24]The constellations were obtained from the free planetarium software Stellarium, ⟨www.stellarium.org⟩.
[25]J. C. Mather *et al.*, "Calibrator design for the COBE far-infrared absolute spectrophotometer (FIRAS)," Astrophys. J. **512**, 511–520 (1999).
[26]For more information on x rays and γ rays we refer the reader to the following missions. X-ray: *ROSAT*, ⟨wave.xray.mpe.mpg.de/rosat⟩, *Chandra*, ⟨chandra.harvard.edu⟩, *XMM-Newton*, ⟨sci.esa.int⟩; γ-ray: *INTEGRAL* ⟨www.esa.int/esaMI/Integral/⟩.
[27]The rotational velocity of a star in a galaxy does not follow Newton's law, but can be read from the rotation curve of the galaxy. See Ref. 28 for the outer rotation curve of the Milky Way.
[28]J. Brand and L. Blitz, "The velocity field of the outer galaxy," Astron. Astrophys. **275**, 67–90 (1993).
[29]The goal of the GAIA mission is to collect high-precision astrometric data for the brightest one billion objects. A detailed description of the ESA Science missions is available at ⟨www.esa.int/esaSC/⟩.
[30]P. Anderson, *Tau Zero* (Orion Publishing Group, London, 2006).
[31]Data are taken from ⟨map.gsfc.nasa.gov⟩.
[32]Single-precision floating-point numbers are stored in a 32 bit word, whereas double-precision ones are stored in a 64 bit word. The word itself is composed of a 23(52) bit mantissa, a 8(11) bit exponent, and one bit for the sign. More information can be found in the IEEE standard for binary floating-point arithmetic for microprocessor systems (ANSI/IEEE Std 754–1985).
[33]This fact is known as the tristimulus theory. For more information see, for example, Foley (Ref. 35).
[34]Color matching functions can be found at the Institute of Ophthalmology, ⟨cvrl.ioo.ucl.ac.uk/basicindex.htm⟩.
[35]J. D. Foley, A. Van Dam, S. K. Feiner, and J. F. Hughes, *Computer Graphics: Principles and Practice* (Addison–Wesley, 1991).
[36]We use the color rendering of spectra by John Walker, ⟨www.fourmilab.ch⟩. The *white point* is the set of chromaticity values (x_w,y_w) that serve to define the *color white*.
[37]An excellent science fiction book on this topic is given in Ref. 30 which might be a useful basis for discussion.